

Transmitter power control for a multicarrier visible light communication system

Christian Kamwangala^{ID} | Mitchell A. Cox^{ID} | Ling Cheng^{ID}

School of Electrical and Information Engineering, University of the Witwatersrand, Johannesburg, South Africa

Correspondence

Ling Cheng, School of Electrical and Information Engineering, University of the Witwatersrand, Johannesburg 2050, South Africa.

Email: ling.cheng@wits.ac.za

Present Address

Ling Cheng, University of the Witwatersrand, 1 Jan Smuts Ave. Braamfontein, Johannesburg 2050, South Africa

Abstract

Higher bandwidth becomes a major challenge in the development and implementation of visible light communication systems as transmission rates increase. One way of increasing bandwidth is through wavelength division multiplexing in multicarrier systems that use red, green, and blue light-emitting diodes to produce white light. However, these systems often suffer from low performance as a result of crosstalk interference, mainly caused by the imperfect nature of optical filters used to discriminate between the colors. This paper demonstrates the use of centralized transmitter power control to predict the trends in the performance of a multicarrier visible light communication system that employs red and blue light emitting diodes. We have shown that, using a model that takes into consideration the effects of optical filters used for detection of colors at the receiver, one is able to predict the trends in the overall system's performance. This enables us to adequately determine the optimal power levels in the red and blue channels, which will result in the best overall performance of the system. Our model can be used in the design and implementation of multicarrier systems to minimize the crosstalk, which improves the performance, and lead to efficient higher bandwidth. The model is first implemented in computer simulations and then tested on an experimental set-up to validate the results.

1 | INTRODUCTION

Radio-based wireless communications are ubiquitous but suffer from several issues, namely, spectrum congestion and lack of bandwidth for future technologies such as fifth generation.^{1,2} In addition, radio transmissions are difficult to secure because the signals easily penetrate through walls. The internet of things will rely heavily on wireless technologies but will cause major congestion on existing wireless infrastructure. LiFi is a potential technology, which uses visible light instead of radio waves for short range wireless communications. With light-emitting diode (LED) lighting becoming common, it is a natural extension of the lighting technology to modulate the LEDs at high speed to enable potentially high bandwidth downlinks.³⁻⁸

In order to further increase the bandwidth of these so-called visible light communication (VLC) systems, wavelength division multiplexing (WDM), which is typically used in fiber optic communications, can be used. As white light can be produced using red, green, and blue (RGB) LEDs, it has been shown that multiplexing of these three colors leads to an increase in bandwidth.⁹⁻¹⁴ Discriminating between the colors in a WDM system is imperfect and is the dominant source of

† **Abbreviations:** VLC, visible light communication; WDM, wavelength division multiplexing; LED, light-emitting diodes; OOK, on off keying

crosstalk, which lowers the capacity of the system due to errors. In this work, we show theoretically and experimentally that a water-filling algorithm can be used to effectively combat this problem.

Resource allocation and coordinated interference management techniques have proved effective in improving the performance of conventional radio communication systems specifically in cognitive radio systems, where systems are affected by high crosstalk interference.¹⁵⁻¹⁹ Application of coordinated interference and resource allocation management techniques such as bit-and-power algorithm to orthogonal frequency-division multiplexing VLC systems have been reported in other works.²⁰⁻²⁵ In this work, we use the water-filling approach to determine the power allocation for a WDM VLC system that employs red and blue LEDs. We are able to predict the trends in the system's bit error rate (BER) and use this information to locate the optimal power allocation point to ensure efficient use of the spectrum. This will result in an improved performance of the WDM system.

The water-filling algorithm is a centralized optimization technique that allows for the adaptation of the transmitter signal to the channel condition to optimize channel capacity. This algorithm is commonly used in radio communication, when the channel is corrupted by strong crosstalk interference or severe fading to improve the transmission rate.^{18,26} More details on how the water-filling algorithm works is given in Section 3 of this report.

In order to adapt this algorithm to the VLC channel, we propose and experimentally verify analytical expressions to determine the power allocation. The total optical power at the transmitter (the total intensity of the red and blue LEDs) is optimally shared between the red and blue subchannels, reducing crosstalk interference between these color subchannels so as to minimize the overall system's BER. Our aim is to be able to find the optimal power allocation point and predict the trends in the overall system's BER, for different power allocations, and investigate how optical filters used at the receiver affect the location of this optimal point. This will enable the design and implementation of more efficient WDM VLC system and further improve the performance of these VLC systems.

In Section 2, a detailed description of the VLC channel is provided with RGB multiplexing in mind. Section 3 presents the formulation of optimal power control for the RGB VLC system based on the water-filling approach. Section 4 describes the analytical solution to the optimization problem for our two color scheme and some simulation results. Thereafter, in Section 5, the experimental set-up is described. Experimental results are presented in Section 6. Concluding remarks are given in Section 7.

2 | CHANNEL MODEL FOR WDM RGB VLC SYSTEMS

In this section, we look at a multicarrier RGB VLC system and consider the main source of crosstalk in these type of system. Consider a WDM RGB-LED VLC system with additive white Gaussian noise channel, as shown in Figure 1. The transmission is governed by Equation (1)^{27,28}

$$\mathbf{r} = \mathbf{H}\mathbf{s} + \mathbf{N}_i = \begin{pmatrix} h_{rr} & h_{rg} & h_{rb} \\ h_{gr} & h_{gg} & h_{gb} \\ h_{br} & h_{bg} & h_{bb} \end{pmatrix} \mathbf{s} + \mathbf{N}, \quad (1)$$

where \mathbf{H} is the 3×3 channel transfer matrix and \mathbf{N} is the subchannel noise vector. \mathbf{r} and \mathbf{s} are 3×1 column vectors that represent the received and transmitted symbols, respectively. The diagonal entries h_{rr} , h_{gg} , and h_{bb} denote the interference free line-of-sight link between a particular LED and its corresponding photodiode where the ideal value is one. The remaining entries represent the cross-talk between the different color subchannels, which are ideally zero.

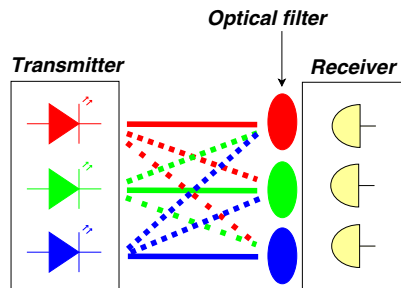


FIGURE 1 Graphical representation of a simple wavelength division multiplexing multicarrier red, green, and blue light-emitting diode visible light communication system corresponding to Equation (1)

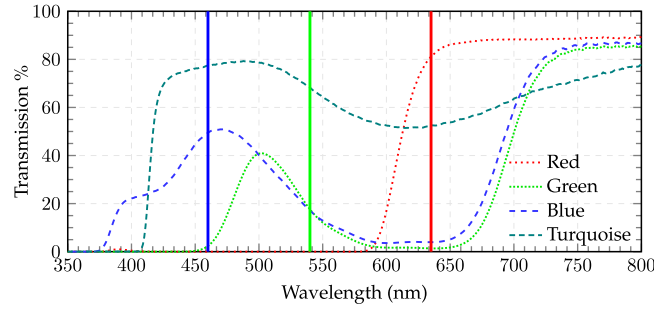


FIGURE 2 Spectrum of the color filters and light-emitting diodes (vertical lines) used in the experiment. The wideband frequency response of the optical filters allows the various color subchannels to interfere with each other, resulting in a poor overall system performance if optimal power control is not used

Detection of RGB light signals at the receiver can be achieved using optical filters to prevent unwanted wavelengths from passing through, while allowing wavelengths of interest. Figure 2 depicts the frequency response obtained from a spectrometer of the different color filters used in the implemented VLC system. Also shown in Figure 2 are the dominant wavelengths of the respective LEDs used.

As can be seen in Figure 2, the imperfect nature of the color filters used at the receiver means that light from the green LED is able to go through the blue filter, while some red light will pass through the green and blue filters.

The signal-to-noise ratio (SNR) in the received signal is dependent on both the shot (and other electronically introduced) noise and background lighting. In this case, however, we assume that another contributor to the SNR is the crosstalk interference between subchannels. Put differently, due to the imperfect nature of the optical filters, each color subchannel is directly affected by the interference from the other subchannels. Therefore, a more accurate expression for SNR should take into account the effects of the interference between the various color subchannels. The SNR can be broken up into three separate expressions for each channel and written as

$$\text{SNR}_R = \frac{|h_{rr}|^2 P_R}{N_o + \Gamma_R}, \quad \text{SNR}_G = \frac{|h_{gg}|^2 P_G}{N_o + \Gamma_G} \quad \text{and} \quad \text{SNR}_B = \frac{|h_{bb}|^2 P_B}{N_o + \Gamma_B}, \quad (2)$$

where P_i is the power of the respective LED N_o is the normalized shot and background noise in the system, and Γ_i is the total interference from the other channels given by

$$\begin{aligned} \Gamma_R &= |h_{rg}|^2 P_G + |h_{rb}|^2 P_B \\ \Gamma_G &= |h_{gr}|^2 P_R + |h_{gb}|^2 P_B \\ \Gamma_B &= |h_{br}|^2 P_R + |h_{bg}|^2 P_G. \end{aligned} \quad (3)$$

Equation (2) shows that the crosstalk interference between the color subchannels increases with increasing transmit optical power. Increasing the total power does not necessarily improve the performance. The expressions for SNR in Equation (2) also show that the interference between the different subchannels increases the total noise power of the system, which, in turn, shifts the detection threshold level away from its optimal level, thus resulting in a reduced system performance.

The probability of error often referred to as BER is the most important metric used to assess the performance of a digital communication system. The BER is a function of the SNR and as OOK is the modulation scheme used in our VLC multicarrier system; the BER is expressed as^{29,30}

$$\text{BER}_{\text{OOK}} = Q\left(\sqrt{\text{SNR}}\right), \quad (4)$$

where $Q(x)$ is the Gaussian complementary error function. Assuming that the bit rate is the same across all color subchannels, in an OOK modulated WDM VLC system with RGB LEDs, the overall BER can be expressed in terms of the individual BER in the red, blue, and green subchannels as

$$\text{BER}_{\text{RGB}} = \frac{1}{3} (\text{BER}_R + \text{BER}_G + \text{BER}_B). \quad (5)$$

The variables BER_R , BER_B , and BER_G in Equation (5) represent the individual BER for the red, blue, and green color subchannels, respectively. The expression for the overall system's BER in Equation (5) can now be written in terms of the Q-function in (4) and the SNR in (2) as

$$\text{BER}_{\text{RGB}} = \frac{1}{3} \left(Q \left(\sqrt{\frac{|h_{rr}|^2 P_R}{N_o + \Gamma_R}} \right) + Q \left(\sqrt{\frac{|h_{gg}|^2 P_G}{N_o + \Gamma_G}} \right) + Q \left(\sqrt{\frac{|h_{bb}|^2 P_B}{N_o + \Gamma_B}} \right) \right). \quad (6)$$

From Equation (6), it is clear that the crosstalk between the color subchannels affects the overall system's BER. Therefore, the use of optimal power control to efficiently allocate the total power at the transmitter to reduce the crosstalk can greatly impact on the performance of the system, which is directly related to the system's BER.

3 | OPTIMAL POWER CONTROL

The available optical power at the transmitter is constrained in an indoor VLC system, due to human eye safety concerns, flickering mitigation, and efforts to reduce power consumption. Various dimming techniques have been proposed to achieve different levels of illuminance when performing different types of activities.¹ In this project, pulse-width-modulation dimming control has been adopted for varying the power levels in the various color subchannels due to its ease of implementation.

Let P_{tot} denote the total available optical power at the transmitter, and then the power constraint in a WDM RGB-LED VLC system can be written as $P_{\text{tot}} = P_R + P_G + P_B$, where P_R , P_G , and P_B are the respective optical power of the RGB channels. As can be seen in Equation (2), the SNR of each color subchannel is affected by the crosstalk interference from the other two color subchannels, which, in turn, is a function of the allocated power in those two channels. Therefore, by efficiently allocating the available optical power at the transmitter and taking into consideration the SNR of the individual channel, the level of interference between the three subchannels (RGB) can be reduced, hence improving the overall performance of the system.

When information about the state of the channel is available and if the channel can be divided into parallel independent subchannels such as in the WDM RGB-VLC, the problem of finding the optimal power allocation can be solved by the water-filling algorithm.¹⁵⁻¹⁸ In the water-filling optimization, each subchannel represents a container that is filled with a certain amount from the total available power considering both noise and interference in the channel.

To better understand how the water-filling algorithm will work in a WDM VLC system, consider the two scenarios in Figure 3. In the first scenario (see Figure 3A), the blue optical filter has a frequency response that allows a large amount of green and red lights to pass through. When transmitter power control is not being used, equal power is allocated to all three subchannels. This creates a lot of crosstalk on the blue subchannel and has a degrading effect on the overall performance of the system. Recall from Equation (2) in Section 2 that the effect of crosstalk in a particular subchannel is dependent on the amount of power in the other two subchannels.

In the second scenario (see Figure 3B), since the red and green optical filters are relatively "good" at keeping out the unwanted signals from the blue LED, we can remedy the effect of crosstalk by taking some power from the red and green subchannels and allocating more power to the blue LED to increase the SNR in the blue subchannel, while at the same time reducing the amount of crosstalk contributed by the green and red subchannels without affecting too much the performance in these two subchannels. This results in a better performance in the blue subchannel, and hence an improved overall system's performance.

The water-filling algorithm is usually formulated in terms of channel capacity. However, channel capacity cannot be directly measured in practice. This requires a different formulation that makes use of BER to assess the improvement made to the system. Assuming that the bit rate is the same across all color subchannels, the power allocation problem can be chosen so as to minimize the rate in Equation (6). Under the power constraint that P_{tot} is a constant, the power allocation problem can be solved by finding the solution to the optimization problem in Equation (7)

$$\text{minimize} \quad \left[\frac{1}{3} \left(Q \left(\sqrt{\frac{|h_{rr}|^2 P_R}{N_o + \Gamma_R}} \right) + Q \left(\sqrt{\frac{|h_{gg}|^2 P_G}{N_o + \Gamma_G}} \right) + Q \left(\sqrt{\frac{|h_{bb}|^2 P_B}{N_o + \Gamma_B}} \right) \right) \right] \quad (7)$$

subject to

$$P_R + P_G + P_B = P_{\text{tot}} \quad \text{and} \quad P_R, P_G, P_B \geq 0. \quad (8)$$

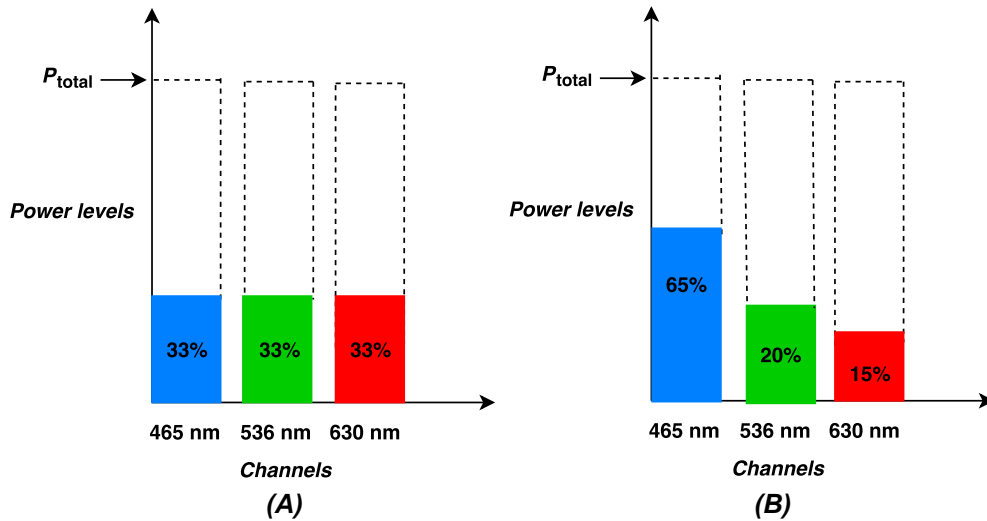


FIGURE 3 An example to illustrate the water-filling power control algorithm for a multicarrier red, green, and blue light-emitting diode visible light communication system. Each color subchannel is viewed as a container and the power levels are determined based on noise and interference to improve overall system performance. Recall from Figure 2 that we have a “bad” blue filter, which allows signals from the green and red subchannels to pass through. In case (A), equal power is allocated to all three subchannels, this creates a lot of crosstalk on the blue subchannel. In case (B), water-filling transmitter power control is used to find the optimal power allocation, which results in better overall system’s performance. This results in an improved performance for the overall system

As explained by the work of Qi et al,¹⁵ the solution to Equation (7) can be solved by the Lagrangian method. Consider the following expression:

$$\mathcal{L}(\lambda, P_R, P_G, P_B) := \text{BER}_{\text{RGB}} - \lambda(P_R + P_G + P_B), \quad (9)$$

where λ is the Lagrange multiplier. Assuming P_i is the transmit power in each color subchannel, the Kuhn-Tucker conditions for optimal solution are

$$\left. \begin{array}{l} \frac{\partial \mathcal{L}}{\partial P_i} = 0 \text{ if } P_i \geq 0 \\ \frac{\partial \mathcal{L}}{\partial P_i} \leq 0 \text{ if } P_i = 0 \end{array} \right\} \text{ where } P_i \in \{P_R, P_G, P_B\}. \quad (10)$$

Once the solution to Equation (9) has been obtained, it will determine the water levels (see Figure 3) for the optimal power allocation. This can then be used to improve the performance of multicarrier WDM VLC systems.

In the next section, we are going to formulate an analytical solution to the optimization problem for a two-channel WDM VLC system that employs red and blue LEDs and uses OOK as the modulation scheme.

4 | SOLUTION TO OPTIMIZATION PROBLEM

In this work, we will consider a general scenario with two colors. The results obtained here can be generalized for application to three colors scheme or any number of wavelengths in WDM VLC systems. In the first part of this section, we look at a VLC system with two color subchannels where there are no optical filters used to discriminate between the wavelengths. We then look at a more realistic scenario where the effects of the optical filters frequency response on the attenuation of the received signals are taken into consideration.

4.1 | Case 1: Normalized channel attenuations

Consider a case where there are no optical filters used at the receiver; all color subchannels attenuations are normalized, and the system noise is uniform across all subchannels. Now, consider a WDM VLC system with two color subchannels, say red and blue. Let the total power in the system $P = P_R + P_B$ be a constant and the bit rate be the same across the two

color subchannels. The objective is to

$$\text{minimize } \left[\frac{Q\left(\sqrt{\frac{P_R}{P-P_R+N_o}}\right) + Q\left(\sqrt{\frac{P-P_R}{P_R+N_o}}\right)}{2} \right], \quad (11)$$

where Q is the Gaussian Q -function defined in Equation (4) and $P_B = P - P_R$. The Gaussian Q -function can be approximated using the CDS approximation as described in the works of Chiani et al²⁹ and Chen and Beaulieu³⁰

$$Q(x) \approx \frac{1}{12} \exp\left(-\frac{x^2}{2}\right) + \frac{1}{4} \exp\left(-\frac{2x^2}{3}\right). \quad (12)$$

Using the expression for the Q -function in Equation (12), a solution to Equation (11) can be found by taking the partial derivative with respect to P_R and equating the result to zero

$$\begin{aligned} \frac{\partial}{\partial P_R} \left(\frac{1}{12} \exp\left(-\frac{P_R}{2(P-P_R+N_o)}\right) + \frac{1}{4} \exp\left(-\frac{2P_R}{3(P-P_R+N_o)}\right) \right. \\ \left. + \frac{1}{12} \exp\left(-\frac{P-P_R}{2(P_R+N_o)}\right) + \frac{1}{4} \exp\left(-\frac{2(P-P_R)}{3(P_R+N_o)}\right) \right) = 0. \end{aligned} \quad (13)$$

Solving for Equation (13) yields the following results:

$$\begin{aligned} \frac{-(P+N_o)}{24(P-P_R+N_o)^2} \exp\left(-\frac{P_R}{2(P-P_R+N_o)}\right) - \frac{1}{6} \frac{P+N_o}{(P-P_R+N_o)^2} \exp\left(-\frac{2P_R}{3(P-P_R+N_o)}\right) \\ + \frac{1}{24} \frac{P+N_o}{(P_R+N_o)^2} \exp\left(-\frac{P-P_R}{2(P_R+N_o)}\right) + \frac{1}{6} \frac{P+N_o}{(P_R+N_o)^2} \exp\left(-\frac{2(P-P_R)}{3(P_R+N_o)}\right) = 0. \end{aligned} \quad (14)$$

Equation (14) shows that one of the stationary point for the cost function in Equation (11) occurs when $P_R = P_B$, ie, when the total available power P is shared equally between the two color subchannels. However, this scenario results in the worst possible BER.

The aforementioned claims can be verified by plotting the cost function in Equation (11) as a function of both P_R and P_B under total power P constraint as illustrated in Figure 4.

From Figure 4, one can see that there exist two other stationary points close to the two extremities. These are global minimums, and they dictate that, to achieve a better overall BER performance in the system, more power must be allocated to one of the subchannels with respect to the other. This is equivalent in practice to using a single subchannel for

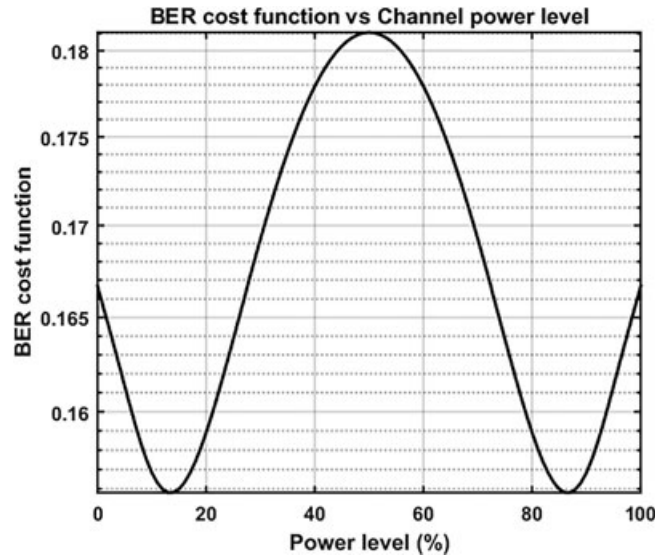


FIGURE 4 Simulated bit-error-rate (BER) cost function as a function of the power levels in the red and blue subchannels with normalized channel attenuations. The two plots are symmetrical and overlay each other. Equal power to the subchannels results in the worst performance at a global maximum, while better performances occur at global minimums close to the extremities where much more power is given to a single subchannel

data transmission. However, this is an extreme case as it is assumed that no optical filters were used at the receiver to discriminate between the different wavelengths.

Most of the work in literature on VLC systems, which use WDM to increase the channel capacity, do not consider the effects of the type of filters used on the performance of such systems. In the next section, we investigate how the type of filters used affect the overall system's performance with respect to the power allocation in the different color subchannels.

4.2 | Case 2: Considering the effects of optical filters

Until now, we have considered an ideal scenario where the respective channel attenuation from the filter have been neglected. In practice, however, detection of RGB signals at the receiver requires using either optical color filters or color sensors. Optical color filters have an absorption coefficient, which affect the SNR of the received signals, and hence results in signal attenuation. The optimization equation can now be written as

$$\text{minimize} \left[\frac{Q\left(\sqrt{\frac{h_{rr}P_R}{h_{rb}(P-P_R)+N_o}}\right) + Q\left(\sqrt{\frac{h_{bb}(P-P_R)}{h_{br}P_R+N_o}}\right)}{2} \right], \quad (15)$$

where the h_{xx} variables represent entries in the transmission matrix \mathbf{H} , such as that defined in Equation (1). These absorption coefficients affect the shape of the cost function in Equation (15), and hence determine the performance of the system for different type of power levels applied to the system.

4.3 | Simulation results

In order to understand how the filters' transmission coefficients affect the optimization cost function in Equation (15), simulations were performed by substituting in the values for h_{rr} , h_{bb} , h_{rb} , and h_{br} as measured for the filters used in the experiment. As an example of a low crosstalk case, the resulting \mathbf{H} matrix for a two-color scheme using red and blue filters from Figure 2 is shown in Equation (16) as follows:

$$\mathbf{H} = \begin{pmatrix} 0.96 & 0.10 \\ 0.16 & 0.88 \end{pmatrix}. \quad (16)$$

It is important to note that as with the previous case, the channel's noise was assumed to be additive white Gaussian noise and has been normalized in these computer simulations. The resulting cost function with respect to the power allocation in the red and blue color subchannels is shown in Figure 5.

The values used for h_{rr} , h_{bb} , h_{rb} , and h_{br} in the cost function of Equation (15) are simply those of the optical filters used in our experimental set-up, which can be read from Figure 2. Figure 5 shows the calculated values for "good" filters, namely, the blue and red, which have minimal crosstalk.

Taking a closer look at the plot in Figure 5 reveals that the optimal power allocation in this case is asymmetrical and does not lie half way between the two color subchannels as would be the case in a naive implementation. That said, because

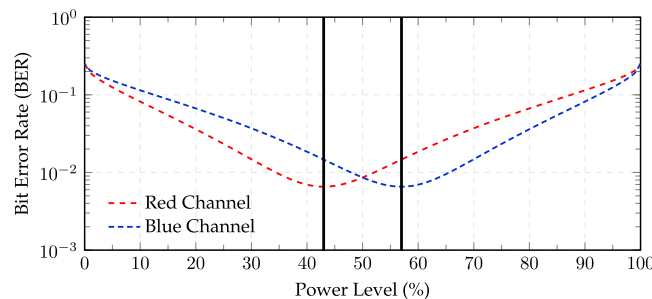


FIGURE 5 Bit-error-rate cost function to illustrate the trend in the system's overall performance as a function of the power allocation in the red and blue channels. This plot shows that the optimal power allocation point lies at 43% for the red subchannel and 57% for the blue. The channel noise was assumed to be additive white Gaussian noise and has been normalized for the simulation. Due to the fact that the total available power in the system is constrained, the two graphs are mirror images of each other in the vertical axis

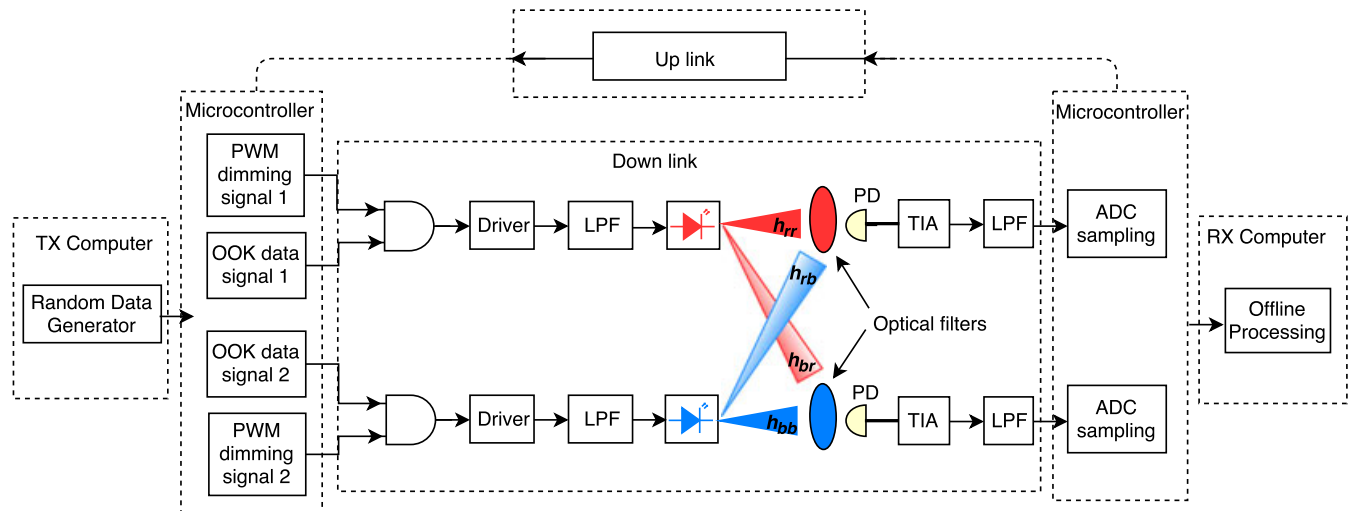


FIGURE 6 Block diagram of the experimental setup for the wavelength division multiplexing visible light communication system. The uplink feedback is used to obtain information about the state of the channel and was implemented in software as a way to simulate a two-way system. ADC, analog-to-digital converter; LPF: low pass filter; OOK, on off keying; PD: photodiode; PWM, pulse width modulation, TIA: transimpedance amplifier

good filters have been used, the allocation is expected to be close to 50%. When higher crosstalk is present, the split will be more significant as shown in the experiment. The calculated optimal power settings are 57% of the total transmitter power for the blue subchannel, while the remaining 43% should be allocated to the red subchannel.

5 | EXPERIMENTAL SET-UP

The experimental set-up of the WDM VLC testbed used in this paper using red and blue LEDs with modulating data over a distance of 1 m optical channel is shown in Figure 6. Our WDM system comprises of discrete red and blue LEDs with wavelength in the regions of 630 nm (red) and 465 nm (blue).

The Cree XLamp XB-D LEDs series was selected. These 3000 mW radiant flux LEDs show a high efficiency of up to 136 lumen/W in cool white (at 85° C, 350 mA), providing a nominal flux of 139 lumen at 25° C. With a maximum driving current of 1 A and a wide viewing angle from 115° to 140°, this is sufficient for data transfer over a distance of 1 m. Modulation bandwidth testing was conducted to assess the switching capability of the LEDs using a square wave, which shows that no distortion occurs up to a frequency of 1 MHz transistor-transistor logic signal input.

The data signals are generated from a computer and fed to a microcontroller unit to drive the two LEDs (red and blue) simultaneously and with the same bit rate. Two independent pulse-width-modulation dimming control signals are also generated by the microcontroller and combined with the data signals to vary the power allocated to each color subchannel. The resulting signals are then used to modulate the LEDs.

At the receiver, optical color filters are used to separate the incoming signals, which are detected using a PIN photodiode with spectral range of sensitivity in the region of 400 nm to 1100 nm. This covers the LEDs used in this project with an active area of 1 mm². By use of a transimpedance amplifier, the output current from the photodiode is converted into a voltage signal that can be sample by the analog-to-digital converter of the microcontroller. The resulting digital data is then fed to the receiving computer for BER analysis and further processing.

The uplink feedback is used to obtain information about the state of the channel related to the h_{xx} values, when different type of filters are used at the receiver. This information is then used to determine the optimal power allocation for the specific type of filters currently used in the system. In the current project, this feedback channel was implemented in software as a way to simulated a two-way system on the experimental set-up.

6 | EXPERIMENTAL METHODOLOGY AND RESULTS

In order to validate the simulation results, the power allocation was implemented on the experimental set-up and tested with different type of filters. The experimental set-up uses optical filters that correspond to the values used for h_{rr} , h_{bb} ,

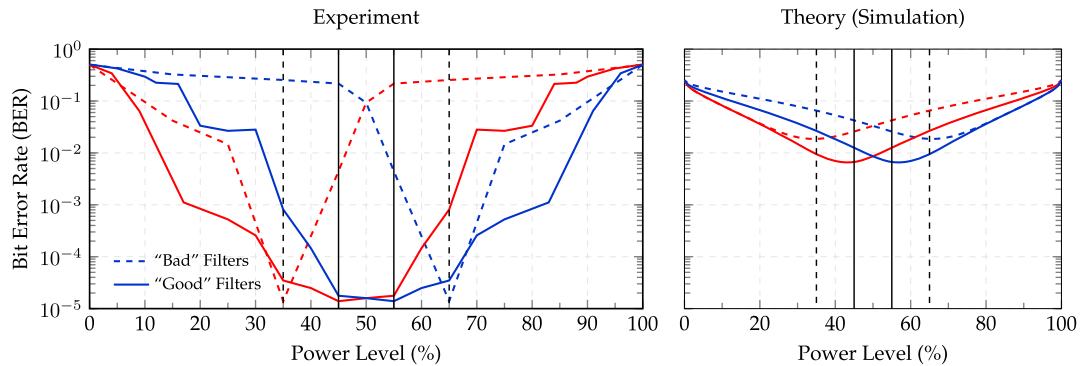


FIGURE 7 Simulations (right) and experimental (left) BER trends as a function of the power allocation in the red and blue subchannels for two different sets of filters. The experimental results closely follow the theoretical predictions in terms of the optimal power allocation. The vertical lines indicate the optimal power allocations based on the experimental results and the discrepancy to the theory is due to the granularity of the experiment

h_{rb} , and h_{br} during simulations. In addition, the data rate across the blue and the red color subchannels was kept the same to ensure uniformity with the computer simulations as per Equation (15). We are interested in the trend of the system's BER as a function of the power allocation, and therefore, for every power allocation in the red and blue subchannels, the corresponding BER was calculated. The same process was repeated with different type of filters to determine how the system behaves under different conditions, and more importantly, how these optical filters affect the location of the optimal operating point. The experimental results are presented in Figure 7.

Figure 7 shows that the experimental results closely follow the same trend as predicted by the simulations. It is important to note the discrepancy between the simulated BER values and the experimental ones. This is due to the fact that, in the computer simulations, the channel noise and attenuations were normalized. We can also see in Figure 7 that, when a set of “good” optical filters (see Figure 2), which have minimal crosstalk, is used on the red and the blue color subchannels, the optimal power allocation point lies closely within the (50 – 50)% mark. However, it can be seen that, when a “bad” filter such as the “turquoise” optical filter (see Figure 2) is used on the blue channel, the optimal power allocation point shifts significantly away from the half-way mark. In this case, a lot more power needs to be allocated to the blue subchannel to compensate for the frequency response of the “turquoise” filter. A similar pattern was observed with other type of red and blue filters. The optical “turquoise” filter use case scenario has been presented here to illustrate the impact that the filters' transmission indexes have on the power allocation.

The objective of this paper was to be able to predict the trend in the system's BER as a function of the power allocation in the red and blue color subchannels, and to assess the impact that the optical filters used, have on the location of the optimal power allocation point. The results in Figure 7 show that the performance of WDM system can be greatly improved by using a power allocation scheme that takes into consideration the frequency response of the optical filters used at the receiver.

Future work and improvement to the model should consider the possibility of predicting the exact BER values in addition to the trends and location of the optimal power point.

7 | CONCLUSION

In this paper, we have shown that using an approach based on the water-filling algorithm, we are able to predict the trend in the overall performance of a WDM VLC system that employs red and blue LEDs. Experimental results show that the optimal power allocation point does not always lie close to the half-way mark, due to the fact that it is dependent on the type of optical filters used to discriminate between the wavelengths. This simplified model, although not yet able to predict the exact BER of the system, can still adequately determine the optimal power levels in the different subchannels, which will result in the best overall performance for the multicarrier VLC system. The results obtained in this paper can be extended to WDM VLC systems with three or any number of wavelengths. Our model can be used in the design and implementation of multicarrier VLC systems to minimize the crosstalk between subchannels. This will improve the performance and lead to efficient higher bandwidth in such systems.

ORCID

Christian Kamwangala  <http://orcid.org/0000-0002-6969-0682>

Mitchell A. Cox  <http://orcid.org/0000-0002-1115-3729>

Ling Cheng  <http://orcid.org/0000-0001-7873-8206>

REFERENCES

1. Pathak PH, Feng X, Hu P, Mohapatra P. Visible light communication, networking, and sensing: a survey, potential and challenges. *IEEE Commun Surv Tutor*. 2015;17(4):2047-2077.
2. O'Brien DC. Visible light communications: Challenges and potential. Paper presented at: IEEE Photonic Society 24th Annual Meeting (PHO 2011); 2011; Arlington, VA.
3. Dimitrov S, Haas H. *Principles of LED Light Communications: Towards Networked Li-Fi*. Cambridge, UK: Cambridge University Press; 2015.
4. Uysal M, Capsoni C, Ghassemloooy Z, Boucouvalas A, Udvary E, eds. *Optical Wireless Communications: An Emerging Technology*. Cham, Switzerland: Springer International Publishing; 2016. *Signals and Communication Technology*.
5. Afgani MZ, Haas H, Elgala H, Knipp D. Visible light communication using OFDM. Paper presented at: 2nd International Conference on Testbeds and Research Infrastructures for the Development of Networks and Communities (TRIDENTCOM 2006); 2006; Barcelona, Spain.
6. Vucic J, Kottke C, Nerreter S, Langer KD, Walewski JW. 513 Mbit/s visible light communications link based on DMT-modulation of a white LED. *J Lightwave Technol*. 2010;28(24):3512-3518.
7. Lee S, Randel S, Breyer F, Koonen MJ. PAM-DMT for intensity-modulated and direct-detection optical communication systems. *IEEE Photonics Technol Lett*. 2009;21(23):1749-1751.
8. Fernando N, Hong Y, Viterbo E. Flip-OFDM for optical wireless communications. Paper presented at: 2011 Information Theory Workshop (ITW), IEEE; 2011; Paraty, Brazil.
9. Chi N, Zhang M, Zhou Y, Zhao J. 3.375-Gb/s RGB-LED based WDM visible light communication system employing PAM-8 modulation with phase shifted Manchester coding. *Opt Express*. 2016;24(19):21663-21673.
10. Wang Y, Huang X, Tao L, Chi N. 1.8 Gb/s WDM VLC over 50-meter outdoor free space transmission employing CAP modulation and receiver diversity technology. Paper presented at: Optical Fiber Communication Conference 2015; 2015; Los Angeles, CA.
11. Wang Y, Huang X, Tao L, Shi J, Chi N. 4.5-Gb/s RGB-LED based WDM visible light communication system employing CAP modulation and RLS based adaptive equalization. *Opt Express*. 2015;23(10):13626-13633.
12. Wang Y, Shao Y, Shang H, et al. 875-Mb/s asynchronous bi-directional 64QAM-OFDM SCM-WDM transmission over RGB-LED-based visible light communication system. Paper presented at: Optical Fiber Communication Conference and Exposition and the National Fiber Optic Engineers Conference 2013; 2013; Anaheim, CA.
13. Wu F, Lin CT, Wei C, et al. Performance comparison of OFDM signal and CAP signal over high capacity RGB-LED-based WDM visible light communication. *IEEE Photon J*. 2013;5(4).
14. Lin W, Chen C, Lu H-H, et al. 10m/500 Mbps WDM visible light communication systems. *Opt Express*. 2012;20(9):9919-9924.
15. Qi Q, Minturn A, Yang Y. An efficient water-filling algorithm for power allocation in OFDM-based cognitive radio systems. Paper presented at: 2012 International Conference on Systems and Informatics (ICSAI 2012); 2012; Yantai, China.
16. Wu J, Yang L, Liu X. Resource allocation based on linear waterfilling algorithm in CR systems. Paper presented at: 7th International Conference on Wireless Communications, Networking and Mobile Computing (WiCOM 2011); 2011; Wuhan, China.
17. Shin WJ, Kim DI. Penalized iterative waterfilling algorithm for multi-cell and multi-user OFDMA systems. Paper presented at: 20th IEEE International Symposium on Personal, Indoor and Mobile Radio Communications, PIMRC; 2009; Tokyo, Japan.
18. Yu W, Cioffi JM. On constant power water-filling. Paper presented at: IEEE International Conference on Communications (ICC 2001); 2001; Helsinki, Finland.
19. Zander J. Performance of optimum transmitter power control in cellular radio systems. *IEEE Trans Veh Technol*. 1992;41(1):57-62.
20. Cogalan T, Haas H, Panayirci E. Power control-based multi-user li-fi using a compound eye transmitter. Paper presented at: 2015 IEEE Global Communications Conference (GLOBECOM 2015); 2015; San Diego, CA.
21. Jin F, Li X, Zhang R, Dong C, Hanzo L. Resource allocation under delay-guarantee constraints for visible-light communication. *IEEE Access*. 2016;4:7301-7312.
22. Wei L, Zhang H, Yu B. Optimal bit-and-power allocation algorithm for VLC-OFDM system. *Electron Lett*. 2016;5(12):1036-1037.
23. Kashef M, Abdallah M, Qaraqe K, Haas H, Uysal M. Coordinated interference management for visible light communication systems. *J Opt Commun Netw*. 2015;7(11):1098.
24. Bykhovsky D, Arnon S. Multiple access resource allocation in visible light communication systems. *J Lightwave Technol*. 2014;32(8):1594-1600.
25. Sun Z, Zhu Y, Zhang Y. The DMT-based bit-power allocation algorithms in the visible light communication. Paper presented at: 2012 2nd International Conference on Business Computing and Global Informatization (BCGIN 2012); 2012; Shanghai, China.
26. Dai M, Zhang S, Chen B, Lin X, Wang H. A refined convergence condition for iterative waterfilling algorithm. *IEEE Commun Lett*. 2014;18(2):269-272.

27. Ndjiongue AR, Ferreira HC, Ngatched TMN. Visible light communications (VLC) technology. In: Webster J. *Wiley Encyclopedia of Electrical and Electronics Engineering*. New York, NY: John Wiley & Sons, Inc; 2015:1-15. ISBN 047134608X.
28. Ndjiongue AR, Ferreira HC, Song J, Yang F, Cheng L. Hybrid PLC-VLC channel model and spectral estimation using a nonparametric approach. *Trans Emerging Tel Tech*. 2017;28(12):e3224.
29. Chiani M, Dardari D, Simon MK. New exponential bounds and approximations for the computation of error probability in fading channels. *IEEE Trans Wirel Commun*. 2003;2(4):840-845.
30. Chen Y, Beaulieu NC. A simple polynomial approximation to the Gaussian Q-function and its application. *IEEE Commun Lett*. 2009;13(2):124-126.

How to cite this article: Kamwangala C, Cox MA, Cheng L. Transmitter power control for a multicarrier visible light communication system. *Trans Emerging Tel Tech*. 2018;e3453. <https://doi.org/10.1002/ett.3453>